

DATA AND CODE AVAILABILITY

All supporting data are available from data repositories. All primary data are available upon request from the corresponding author or trial sponsor.

SUPPLEMENTARY RESULTS

Safety Profile of CD14 Blockade with Anti-CD14 Antibody

No adverse events were observed following anti-CD14 treatment commencement (**Supplementary Table S1**). Left atrial thrombus was observed in one mouse in the isotype-treated group only (7-days post-STEMI cohort).

Model of Reperfused Anterior STEMI Develops Progressive LV Systolic Dysfunction, Remodeling, and Hemodynamic Decompensation following STEMI

Following 1 h of LAD coronary artery occlusion and closed chest reperfusion, hearts had an AAR comprising approximately 50 % of the total LV (see **Supplementary Figure S3B-D**), and hearts of saline-treated control mice developed an acute infarct size of 65 ± 4 (% of AAR) measured by planimetric analysis of serially sectioned and dual-stained (by Evans blue/tri-tetrazolium chloride) whole hearts excised 24 h post-STEMI (**Supplementary Figure S3C**). At 24 h post-STEMI, untreated mice exhibited depressed LV systolic function (29 ± 2 % EF) with evidence of early adverse remodeling i.e. increased end-diastolic volume (74 ± 3 μ l EDV), observed by ultra-high frequency parasternal long axis echocardiography (**Supplementary Figure S3E-I**), partially associated with acute myocardial stunning.

At 3 days post-STEMI, untreated mice presented with similar LV systolic dysfunction (31 ± 1 % EF) and dilatation (74 ± 3 μ l EDV, **Supplementary Figure S3J-N**).

At 7 days post-STEMI without treatment, LV dilatation remained stable (77 ± 3 vs 74 ± 3 μ l EDV at D3 post-STEMI, $p=0.549$). However, systolic dysfunction progressively worsened without treatment (25 ± 1 vs 31 ± 1 % EF at D3 post-STEMI, $p<0.001$) alongside reduced LV stroke volume (19 ± 1 vs 23 ± 1 μ l at D3,

p<0.01) and cardiac output (9.9 ± 0.4 vs 12.5 ± 0.5 ml/min at D3, p<0.001) (**Figure 2B, text**). Invasive hemodynamics were similarly impacted at 7 days post-STEMI, including significantly reduced developed pressure (i.e. delta between end-systolic end-diastolic LV pressure; 78 ± 2 vs 92 ± 3 mmHg in shams, p<0.05), and approximately halved LV stroke work ($1,103\pm63$ vs $2,075\pm309$ mmHg x μ l in shams, p<0.001), assessed by LV pressure-volume (PV) catheterization (**Figure 2C, text**).

At 21 days post-STEMI, cardiac magnetic resonance (CMR) imaging provided an additional assessment of LV volumes, further validating echocardiographic observations of LV dilatation without treatment (i.e. 102 ± 8 μ l in saline controls). At 28 days, echocardiography showed that LV systolic dysfunction had remained depressed but stable compared with day 7 (24 ± 1 vs $25\pm2\%$ EF at D7 post-STEMI, p=0.560), alongside progressive LV dilatation (111 ± 6 vs 77 ± 3 μ l EDV at D7 post-STEMI, p<0.001, **Figure 2F, text**). Global longitudinal strain (GLS) of the LV was also suppressed at this timepoint (-6.8 ± 0.3 vs $-12.6\pm0.7\%$ in shams, p<0.001). As observed at day 7 post-STEMI, LV developed pressure remained depressed at 28 days (80 ± 2 vs 91 ± 2 mmHg in shams, p<0.01) with the additional development of reduced +dP/dT ($6,902\pm248$ vs $9,446\pm497$ in shams, p<0.01) and -dP/dT ($-5,928\pm476$ vs $-8,737\pm443$ in shams, p<0.01) at this timepoint (**Figure 2G, text**).

Together these changes are reflected in a shrinking and overt rightward shift of the PV loop between days 7 and 28 in this model of murine STEMI (**Figure 2**). In our extensive experience with this model, no significant additive functional decompensation or remodeling is observed beyond 28 days post-STEMI.

1 SUPPLEMENTARY TABLES AND FIGURES

| Adverse Events | Saline (n=76) | Isotype (n=66) | Anti-CD14 (n=102) |
|-----------------------------------|------------------|-------------------|----------------------|
| Atrial thrombus (%) | 0 (0%) | 1 (1.5%) | 0 (0%) |
| Cardiac rupture (%) | 0 (0%) | 0 (0%) | 0 (0%) |
| Lung congestion (%) | 0 (0%) | 0 (0%) | 0 (0%) |
| Aneurism (%) | 0 (0%) | 0 (0%) | 0 (0%) |
| Evidence of infection (%) | 0 (0%) | 0 (0%) | 0 (0%) |
| Death or emergency euthanasia (%) | 0 (0%) | 0 (0%) | 0 (0%) |

2 **Supplementary Table S1. Safety and Adverse Events.** Including all observations at post-mortem in animals that
3 survived 1 h ischemia and received any treatment by intravenous injection at time of reperfusion.

4

5

| Stain or Antibody | Supplier (Cat #) |
|---------------------|---|
| Masson's trichrome | Sigma-Aldrich, Stenheim, DE (HT15) |
| Picrosirius red | Sigma-Aldrich, Stenheim, DE (2610-10-8) |
| Anti-CD68 | Abcam, Waltham, Waltham, US (Ab125212) |
| Anti-troponin T | ThermoFisher Scientific, Grand Island, US (MA5-12960) |
| DAPI, hydrochloride | ThermoFisher Scientific, Grand Island, US (D1306) |

6 **Supplementary Table S2. (Immuno)histochemical approach and reagents**

| Cell type | Antibody signature (staining pattern) |
|------------------------------|--|
| Viable Leukocytes | CD45+ |
| Granulocytes | CD45+, CD11b+, Ly6G+ |
| Macrophages | CD45+, CD11b+, CD64+ |
| CD14+ Macrophages | CD45+, CD11b+, CD64+, CD14+ |
| CD14- Macrophages | CD45+, CD11b+, CD64+, CD14- |
| MHCII-hi Macrophages | CD45+, CD11b+, CD64+, MHCII+ |
| MHCII-hi Mrc1+ Macrophages | CD45+, CD11b+, CD64+, MHCII+, MRC1+ |
| MHCII-low; Mrc1+ Macrophages | CD45+, CD11b+, CD64+, MHCII-, MRC1+ |
| MHCII-low Macrophages | CD45+, CD11b+, CD64+, MHCII- |
| Myeloids | CD45+, CD11b+, Ly6G- |
| Non-myeloids | CD45+, CD11b-, Ly6G- |

1 Supplementary Table S3. Leukocyte subtype staining patterns

2

| <i>Flow cytometry</i> | | | | | |
|------------------------------|---------------------|-------------|------------------------------|--------------|-----------------|
| <u>Antibody</u> | | | | | Final |
| <u>Target</u> | Dye | Cat# | Company | Clone | Dilution |
| CD45 | APC-Cy7 | 561037 | BD Biosciences, San Jose, US | 30-F11 | 1:400 |
| I-A/I-E (MHCII) | OptiBuild BUV395 | 743876 | BD Biosciences | 2G9 | 1:400 |
| CD11b | Horizon BUV737 | 612801 | BD Biosciences | M1/70 | 1:400 |
| CD14 | Brilliant violet | 123337 | Biolegend, San Diego, US | Sa14-2 | 1:200 |
| Ly-6C | FITC | 128005 | Biolegend | HK1.4 | 1:400 |
| Ly-6G | PE/dazzle | 127647 | Biolegend | 1A8 | 1:200 |
| CD64 (a & b alloantigens) | PE/cyanine7 | 139313 | Biolegend | X54- 5/7.1 | 1:200 |
| CD206 (Mrc1) | AF647 | 141711 | Biolegend | C068C2 | 1:200 |
| N/A (nucleus) | DAPI (1 mg/mL) | D9542 | Sigma Aldrich | N/A | 1:1000 |
| <i>scRNA-seq</i> | | | | | |
| <u>Antibody</u> | | | | | Final |
| <u>Target</u> | Dye | Cat# | Company | Clone | Dilution |
| CD45 | APC-Cy7 | 561037 | BD Biosciences | 30-F11 | 1:400 |
| CD11b | Horizon BUV737 | 612801 | BD Biosciences | M1/70 | 1:400 |
| CD64 | PE/cyanine7 | 139313 | Biolegend | X54- 5/7.1 | 1:200 |
| N/A (nucleus) | DAPI (1 mg/mL) | D9542 | Sigma Aldrich | N/A | 1:1000 |

1 **Supplementary Table S4. Antibodies used in Flow Cytometry and scRNAseq experiments.**

2

3

4

| Cytokine | Day 1 post-STEMI | | | | Day 3 post-STEMI | | | | Day 1 vs Day 3 | | |
|---------------|--------------------------------|-------------------------------|-------------------------------|---------|-------------------------------|-------------------------------|-------------------------------|---------|-------------------|--------------------|----------------------|
| | Saline (n=10) | Isotype (n=12) | Anti-CD14 (n=11) | p-value | Saline (n=20) | Isotype (n=20) | Anti-CD14 (n=20) | p-value | Saline p-value | Isotype p-value | Anti-CD14 p-value |
| Eotaxin | 441.86 (417.87- 585.74) | 472.42 (412.23- 548.58) | 464.41 (432.69- 543.11) | 0.9521 | 561.11 (465.12- 623.31) | 584.26 (494.99- 649.69) | 534.07 (478.73- 600.95) | 0.5730 | 0.4671 | 0.0630 | 0.2828 |
| G-CSF | 785.92 (623.33- 1099.86) | 768.05 (560.61- 996.63) | 711.39 (594.12- 945.79) | 0.9574 | 319.96 (280.25- 424.99) | 315.3 (258.52- 408.36) | 307.32 (247.85- 402.96) | 0.6456 | <0.0001 | <0.0001 | 0.0030 |
| GM-CSF | 31.42 (26.34- 39.88) | 40.78 (27.77- 46.95) | 31.37 (24.21- 43.22) | 0.2321 | 53.07 (50.56- 54.98) | 53.07 (51.16- 54.33) | 52.03 (50.02- 54.02) | 0.7098 | <0.0001 | <0.0001 | <0.0001 |
| IFN γ | 4.3 (3.86- 7.26) | 6.63 (3.96- 8.59) | 4.89 (3.51- 7.08) | 0.4033 | 10.99 (9.72- 11.38) | 10.8 (10.07- 12.18) | 10.57 (9.77- 11.56) | 0.8542 | <0.0001 | <0.0001 | <0.0001 |
| IL-1 α | 312.12 (271.34- 404.27) | 375.78 (301.31- 396.96) | 328.44 (262.47- 395.71) | 0.6992 | 436.39 (415.04- 455.32) | 451.43 (433.48- 471.39) | 434 (414.34- 461.21) | 0.2138 | 0.0001 | 0.0008 | <0.0001 |
| IL-1 β | 21.46 (19.07- 32.89) | 32.2 (20.85- 40.71) | 25.48 (18.15- 33.24) | 0.4256 | 47.85 (45.98- 51.22) | 49.21 (47.17- 52.25) | 46.99 (45.05- 49.36) | 0.1614 | <0.0001 | <0.0001 | <0.0001 |

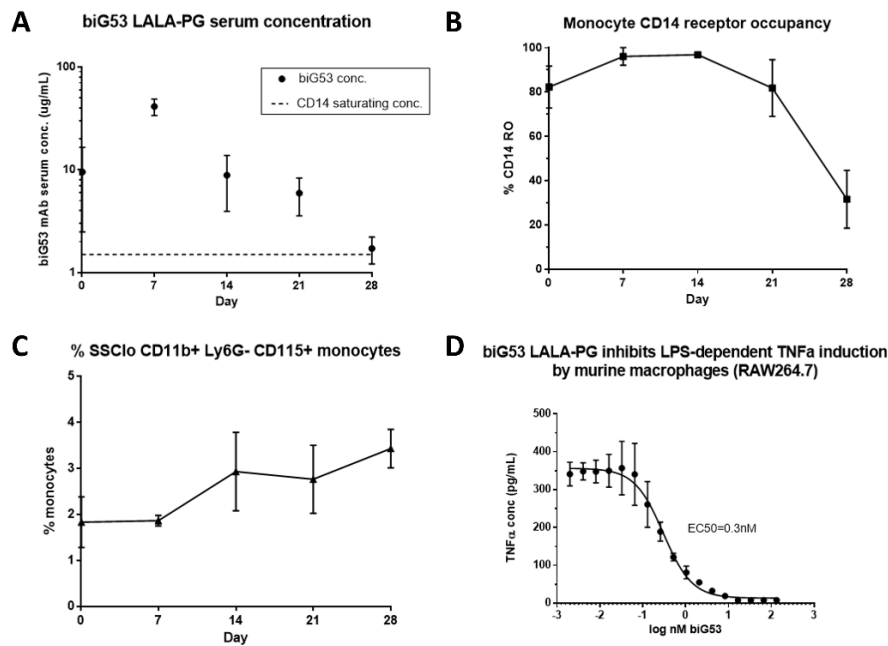
| | | | | | | | | | | | |
|-------|------------------------|--------------------------|--------------------------|--------|---------------------------|---------------------------|---------------------------|--------|-------------------|-------------------|-------------------|
| IL-2 | 56.53 (51.54-74.45) | 69.29 (53.09-77.67) | 64.62 (51.15-73.23) | 0.7123 | 88.74 (85.62-90.71) | 88.68 (86.93-91.43) | 87.25 (86.11-90.52) | 0.5832 | <0.0001 | <0.0001 | <0.0001 |
| IL-3 | 4.44 (3.81-6.74) | 6.8 (3.79-7.9) | 4.47 (3.6-6.79) | 0.2894 | 10.09 (9.49-10.51) | 10.11 (9.19-10.51) | 10.12 (9.45-10.36) | 0.9708 | <0.0001 | <0.0001 | <0.0001 |
| IL-4 | 2.11 (1.65-3.05) | 3.24 (1.91-3.61) | 2.28 (1.63-3.18) | 0.1614 | 3.94 (3.88-4.09) | 4 (3.82-4.17) | 3.9 (3.79-4.15) | 0.7824 | 0.0012 | 0.0004 | <0.0001 |
| IL-5 | 9.8 (7.2-13.47) | 12.24 (10.13-15.95) | 8.92 (8.09-11.44) | 0.0590 | 24.01 (17.61-32.65) | 21.72 (14.45-34.23) | 27.94 (21.07-42.28) | 0.3681 | <0.0001 | 0.0100 | <0.0001 |
| IL-6 | 37.72 (18.42-81.49) | 42.02 (32.59-49.45) | 39.02 (18.79-114.57) | 0.9844 | 40.53 (22.97-56) | 30.29 (19.98-56.05) | 32.31 (24.26-66) | 0.6089 | >0.9999 | 0.9109 | 0.9708 |
| IL-7 | 12.31 (7.78-17.95) | 15.88 (8.13-20.13) | 15.14 (9.93-17.3) | 0.6637 | 26.41 (23.83-28.65) | 26.67 (25.71-28.21) | 26.54 (25.47-30.09) | 0.7574 | <0.0001 | <0.0001 | <0.0001 |
| IL-9 | 78.47 (73.4-105.07) | 117.48 (65.89-123.11) | 106.01 (68.54-122.23) | 0.8153 | 142.86 (137.88-149.36) | 144.59 (138.02-151.28) | 141.79 (136.45-148.89) | 0.7194 | <0.0001 | <0.0001 | <0.0001 |
| IL-10 | 21.35 (16.35-31.2) | 29.56 (17.4-41.26) | 23.95 (15.29-33.27) | 0.4477 | 44.37 (42.01-48.09) | 45.49 (42.85-47.69) | 44.81 (41.51-47.2) | 0.4331 | <0.0001 | 0.0002 | <0.0001 |

| | | | | | | | | | | | |
|----------|-------------------------------|-------------------------------|-------------------------------|--------|-------------------------------|-------------------------------|-------------------------------|--------|-------------------|-------------------|-------------------|
| IL-12p40 | 39.36 (35.78- 63.87) | 56.73 (34.78- 75.92) | 47.68 (33.48- 60.34) | 0.4315 | 84.82 (81- 90.38) | 86.61 (81.62- 92.58) | 81.35 (77.6- 90.66) | 0.5304 | <0.0001 | 0.0001 | <0.0001 |
| IL-12p70 | 123.92 (104.03- 170.74) | 158.22 (121.12- 186.97) | 126.27 (104.71- 170.51) | 0.4441 | 220.91 (210.49- 232.8) | 219.22 (213.52- 227.31) | 214.07 (205.49- 221.9) | 0.3504 | <0.0001 | <0.0001 | <0.0001 |
| IL-13 | 58.13 (48.14- 77.92) | 71.79 (51.44- 84.16) | 62.85 (51.56- 75.16) | 0.5241 | 102.34 (97.66- 105.96) | 100.06 (96.16- 104.69) | 98.86 (94.25- 100.48) | 0.2844 | <0.0001 | <0.0001 | <0.0001 |
| IL-15 | 150.97 (122.38- 182.35) | 172.4 (115.34- 207.99) | 185.66 (149.7- 237.05) | 0.2452 | 247.56 (238.01- 261.26) | 258.07 (245.49- 280.4) | 271.79 (251.38- 281.36) | 0.0882 | <0.0001 | <0.0001 | 0.0016 |
| IL-17 | 2.37 (2- 3.59) | 3.45 (2.07- 4.1) | 2.64 (1.87- 3.72) | 0.4766 | 5.04 (4.57- 5.19) | 5.02 (4.73- 5.1) | 4.71 (4.53- 4.98) | 0.0854 | <0.0001 | <0.0001 | <0.0001 |
| IP-10 | 26.53 (21.75- 31.34) | 29.29 (25.15- 35.02) | 27.81 (22.23- 34.52) | 0.4335 | 27.16 (25.52- 31.09) | 28.55 (24.67- 32.78) | 29.37 (27.26- 33.13) | 0.5719 | 0.8151 | 0.9109 | 0.9708 |
| KC | 150.22 (121.55- 302.35) | 168.09 (117.51- 210.73) | 120.22 (102.27- 181.92) | 0.6917 | 185.48 (132.38- 306.53) | 149.81 (121.72- 190.76) | 178.51 (115.63- 264.11) | 0.3501 | 0.8549 | 0.9542 | 0.8516 |
| LIF | 4.21 (3.31- 5.66) | 4.9 (2.99- 6.46) | 5.05 (3.87- 5.98) | 0.7914 | 7.65 (7.22- 7.8) | 7.99 (7.52- 8.47) | 7.76 (7.41- 8.12) | 0.2807 | 0.0008 | <0.0001 | <0.0001 |

| | | | | | | | | | | | |
|----------------|-------------------------------|--------------------------------|--------------------------------|--------|-------------------------------|-------------------------------|-------------------------------|--------|-------------------|-------------------|-------------------|
| LIX | 348.07 (230.2- 924.41) | 582.33 (169.94- 1102.93) | 398.24 (207.68- 1047.17) | 0.9800 | 278.43 (226.66- 377.98) | 323 (214.93- 590.62) | 319.71 (233.55- 447.98) | 0.7398 | 0.8151 | 0.9109 | 0.8733 |
| MCP-1 | 131.7 (115.11- 147.56) | 150.22 (117.9- 171.54) | 126.99 (116.19- 161.91) | 0.3818 | 183.06 (175.08- 187.48) | 182.42 (172.95- 192.35) | 183.38 (172.37- 195.57) | 0.8488 | <0.0001 | 0.0018 | <0.0001 |
| M-CSF | 48.63 (40.01- 75.08) | 64.62 (43.18- 87.57) | 52.72 (40.71- 70.71) | 0.4752 | 96.87 (92.66- 101.55) | 96.74 (92.45- 101.09) | 93.67 (89.89- 100.51) | 0.4850 | <0.0001 | 0.0046 | <0.0001 |
| MIG | 150.19 (42.4- 308.31) | 148.77 (47.77- 416.27) | 128.46 (41.81- 240.62) | 0.8543 | 62.76 (50.41- 138.07) | 82.44 (62.6- 129.66) | 94.67 (60.64- 151.14) | 0.3475 | 0.8549 | 0.8610 | 0.9708 |
| MIP-1 α | 105.63 (89.16- 123.91) | 115.44 (104.59- 124.32) | 97.76 (89.66- 119.51) | 0.2167 | 128.52 (122.73- 134.21) | 129.5 (126.16- 132.69) | 129.68 (124.78- 132.38) | 0.8816 | 0.0184 | 0.0046 | <0.0001 |
| MIP-1 β | 107.29 (96.8- 116.2) | 120.44 (109.01- 140.75) | 102.56 (91.24- 124.49) | 0.1280 | 132.67 (127.16- 137.48) | 133.28 (129.28- 143.74) | 139.43 (127.83- 143.89) | 0.4032 | <0.0001 | 0.2846 | 0.0014 |
| MIP-2 | 315.87 (292.56- 400.26) | 398.1 (298.77- 431.24) | 342.46 (291.89- 399.89) | 0.4428 | 469.91 (459.66- 485.63) | 469.27 (453.82- 482.34) | 469.29 (450.64- 479.18) | 0.6822 | <0.0001 | <0.0001 | <0.0001 |
| RANTES | 21.24 (18.3- 26.54) | 26.44 (20.57- 30.92) | 25.59 (19.86- 29.89) | 0.4891 | 35.91 (34.83- 38.51) | 36.37 (34.34- 37.99) | 36.27 (35.11-38) | 0.9473 | <0.0001 | <0.0001 | <0.0001 |

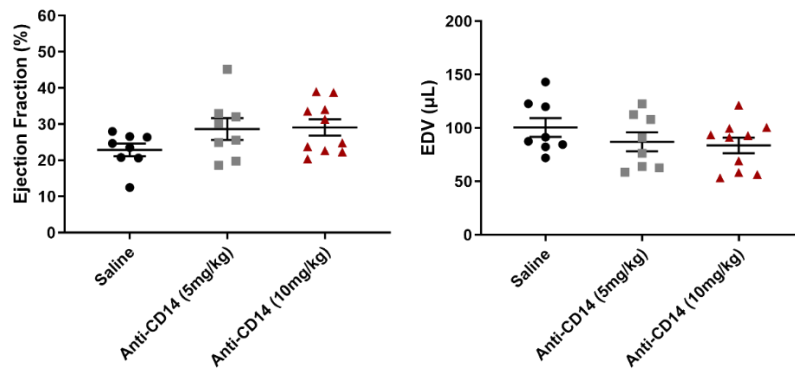
| | | | | | | | | | | | |
|--------------|----------------------------|----------------------------|---------------------------|--------|---------------------------|----------------------------|----------------------------|--------|-------------------|-------------------|-------------------|
| | | | | | | | | | | | |
| TNF α | 19.81 (17.83- 26.87) | 26.44 (19.23- 31.13) | 20.73 (18.89- 28.8) | 0.2128 | 33.5 (31.96- 35.34) | 34.17 (32.89- 35.28) | 33.02 (31.79- 34.23) | 0.1627 | <0.0001 | <0.0001 | <0.0001 |
| VEGF | 1.41 (1.17- 1.92) | 1.83 (1.27- 2.13) | 1.36 (1.14- 1.86) | 0.2408 | 2.41 (2.28- 2.53) | 2.46 (2.37- 2.53) | 2.44 (2.31- 2.56) | 0.7974 | <0.0001 | <0.0001 | <0.0001 |

- 1 **Supplementary Table S5. Circulating growth factor and cytokine levels following CD14 Blockade at D1 and D3 post-STEMI.** Biomarker concentrations in pg/ml. Data
- 2 presented as median (Q1-Q3), with Mann-Whitney U-test conducted between D1 and D3 and Kruskal Wallis test to compare between the three groups at each timepoint.



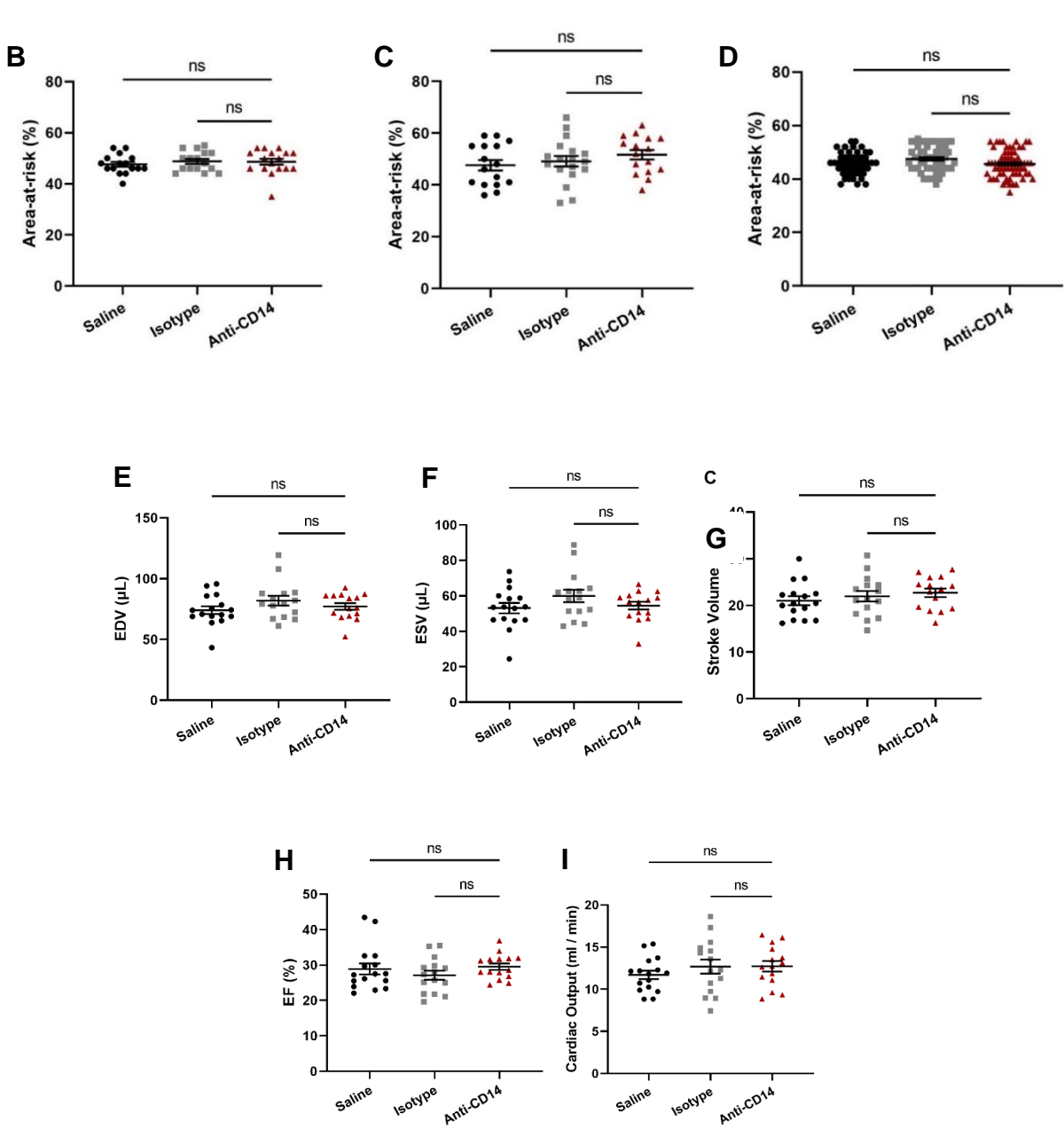
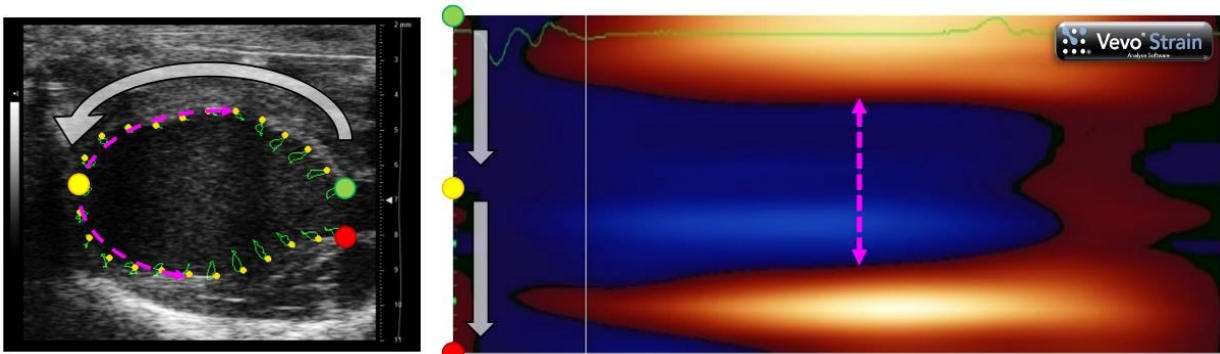
Supplementary Figure S1. Anti-CD14 serum PK, CD14 receptor occupancy, and monocyte frequency

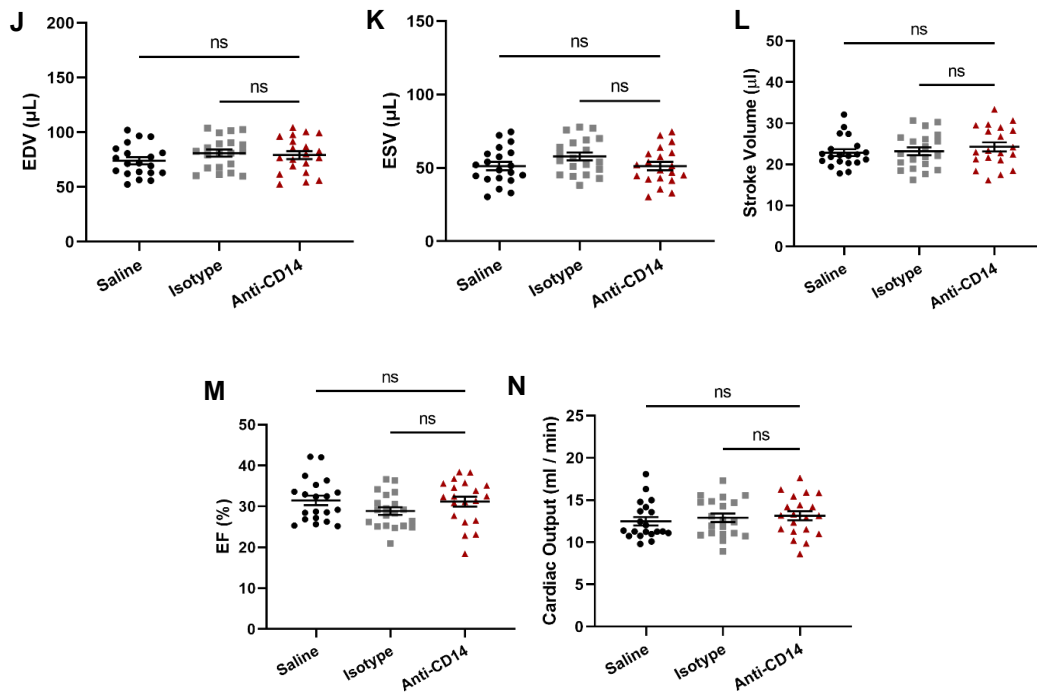
following a 5 mg/kg anti-CD14 mAb infusion. C57BL6 mice (n=3) received a 5 mg/kg infusion of biG53 LALA-PG mAb (anti-CD14) at day 0, with serum and whole blood collection at 0.5 h, 7-, 14-, 21-, and 28-days post-injection. WinNonlin analysis of anti-CD14 serum levels determined a terminal antibody half-life of 160 h. A) A single 5 mg/kg infusion of anti-CD14 achieves serum concentrations necessary for monocyte CD14 saturation (i.e. 1.5 ug/mL) for ~28 days. *In vitro* titration of anti-CD14 on C57BL6 whole blood, followed by monocyte CD14 receptor occupancy (RO) analysis by flow cytometry demonstrated monocyte CD14 saturation is reached at 1.5 ug/mL (dashed line). B) Monocyte CD14 RO as determined by flow cytometry was 96% over 14 days post-infusion. C) A 5 mg/kg infusion of anti-CD14 does not deplete the SSC lo, CD11b+, Ly6G-, CD115+ population as determined by flow cytometry. Graphed values show the mean and standard deviation. D) anti-CD14 blocks LPS-dependent TNF- α secretion in vitro by RAW264.7 cells stimulated with 10 ng/mL LPS. Complete inhibition of TNF- α secretion is achieved at anti-CD14 concentration of 1.5 ug/mL (i.e. 10 nM), the antibody concentration that saturates monocyte CD14 in whole blood. Mean \pm SEM.



Supplementary Figure S2. Echocardiographic results of drug dose comparison pilot study measured 7 days

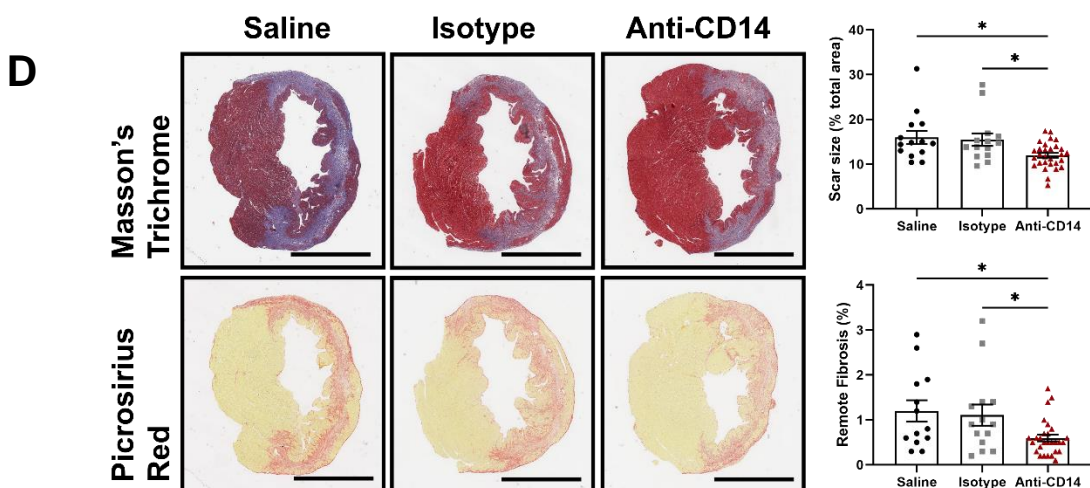
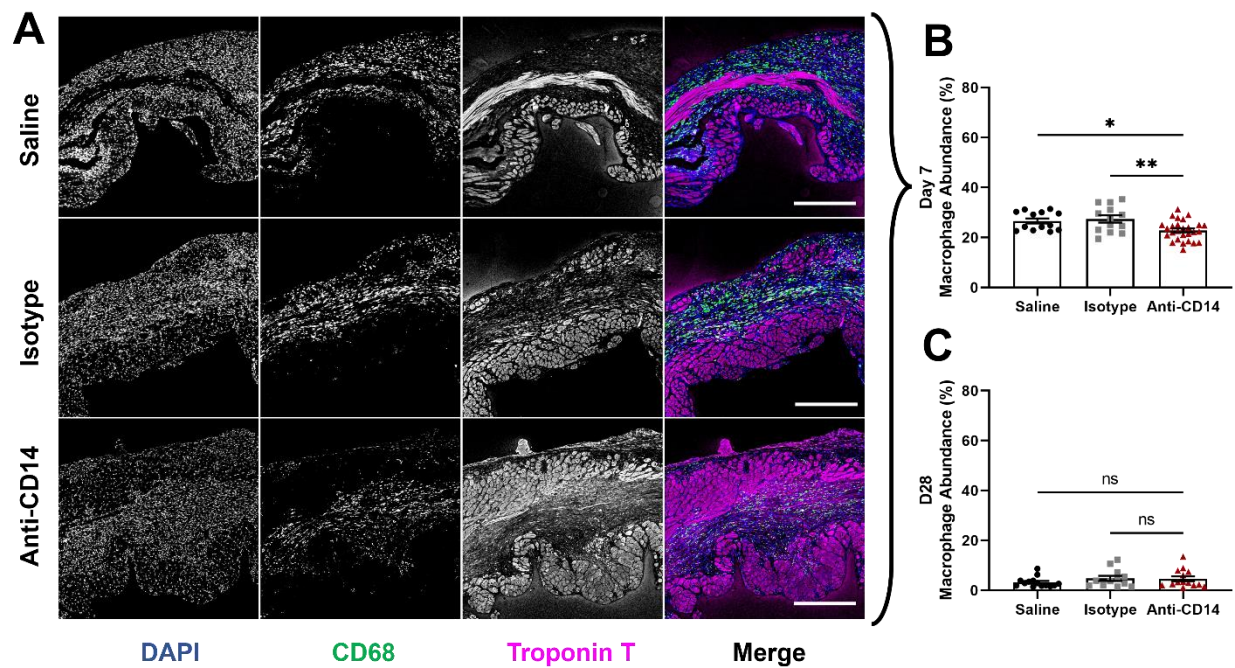
post-STEMI. A small pilot study was designed to confirm systolic function (ejection fraction) effect signal; and determine effect size, standard deviation, and lowest effective dose of anti-CD14 antibody treatment delivered using the same protocols used in the main study i.e. administered intravenously at reperfusion, following 1 h occlusion of the left ventricular left anterior descending coronary artery. EDV – end-diastolic volume. No statistical comparisons were performed in this study.



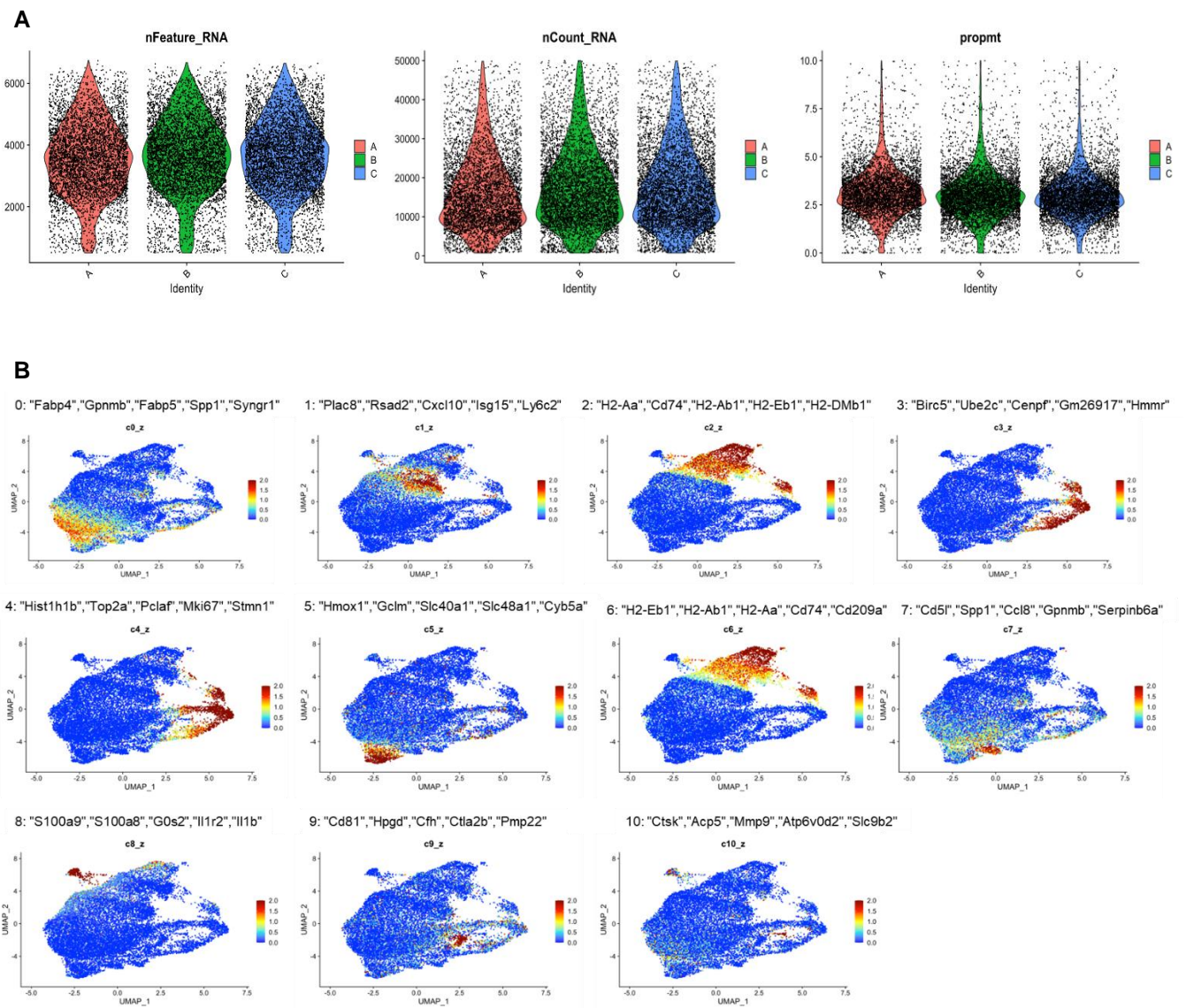


Supplementary Figure S3. Echocardiographic assessments at 24 hours and 3 days post-STEMI.

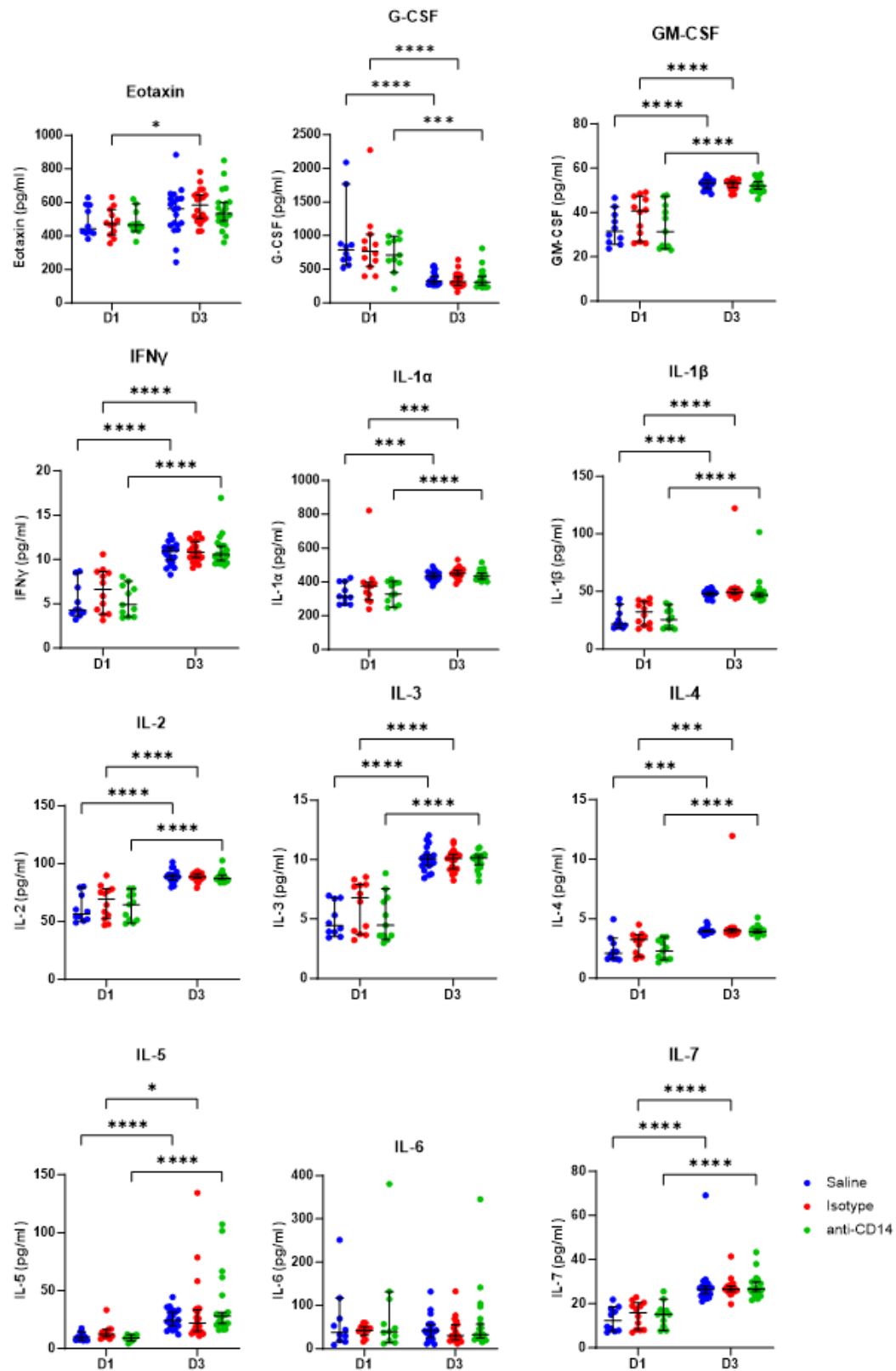
A) Relative wall displacement mapping method for assessing area-at-risk. The endocardial circumference was traced to track (left) and map (right) relative tissue displacement in a single cardiac cycle (note EKG overlay, green). Colored circles at the endocardium in B-mode correlate with those fit to the y-axis on the displacement map. The pink line denotes inactive/negative endocardial wall displacement (blue area in map). Left Ventricular Area-at-risk (AAR) at 24 h post-STEMI measured by B) *in vivo* echocardiography, and C) planimetric assessment following post-mortem excision and EB/TTC dual staining of the same hearts. D) Left Ventricular Area-at-risk (AAR) at 24 h post-STEMI across all studies, measured by *in vivo* echocardiography, demonstrating consistency of AAR between groups across all studies. Further echocardiographic assessments at 24 h post-STEMI included left ventricular volumes (E-G), systolic function (H), and cardiac output (I). Echocardiographic assessments at 3 days post-STEMI included left ventricular volumes (J-L), systolic function (M), and cardiac output (N). EDV – end-diastolic volume, ESV – end-systolic volume, EF – ejection fraction, ns – not significant. Mean ± SEM.



Supplementary Figure S4. Immunofluorescent imaging of myocardial infiltrates of monocytes and macrophages and histological assessment of fibrosis at 7- or 28-days post-STEMI. A) Representative immunofluorescent images and B) relative abundance of CD68+ cells in the infarcted myocardium 7 days post-STEMI. C) Relative abundance of CD68+ cells 28 days post-STEMI. D) Representative histological images of Masson's trichrome (upper panels) and picrosirius red (lower panels, bars 500 μ m) at 7 days post-STEMI, and assessments of scar size (free wall lesion percentage of total area) and remote (non-lesion/septal) fibrosis. Mean \pm SEM. *p<0.05, **p<0.01, ns - not significant.



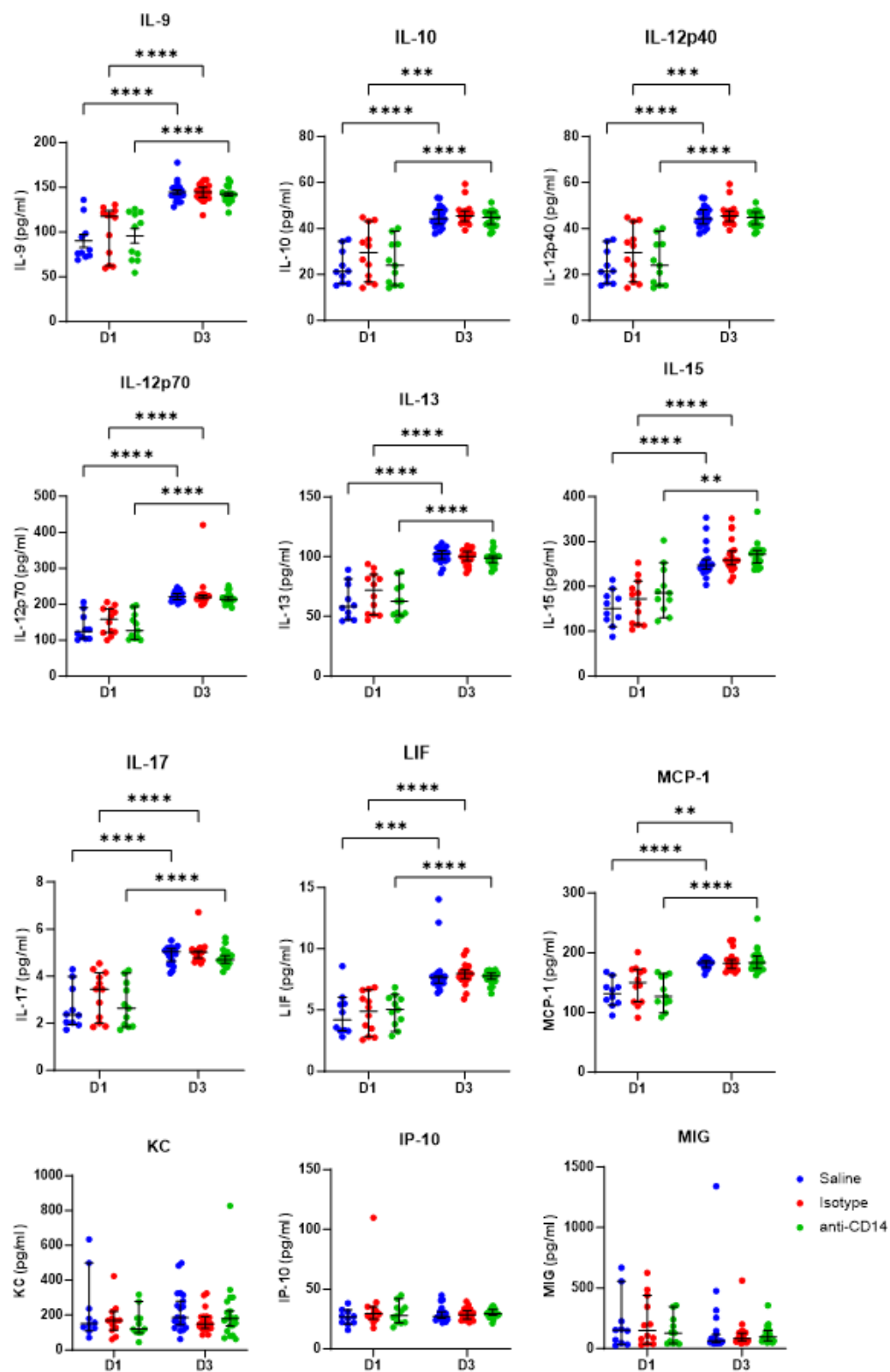
Supplementary Figure S5. Assessments of scRNAseq data quality. A) Quality control assessments performed on blinded/de-identified groups (A – isotype, B – Anti-CD14, C – Saline). B) Marker gene set z-scores for myeloid cell states (Clusters).



1

2 Supplementary Figure S6. Circulating Growth Factor and cytokine levels following CD14 Blockade at D1 and

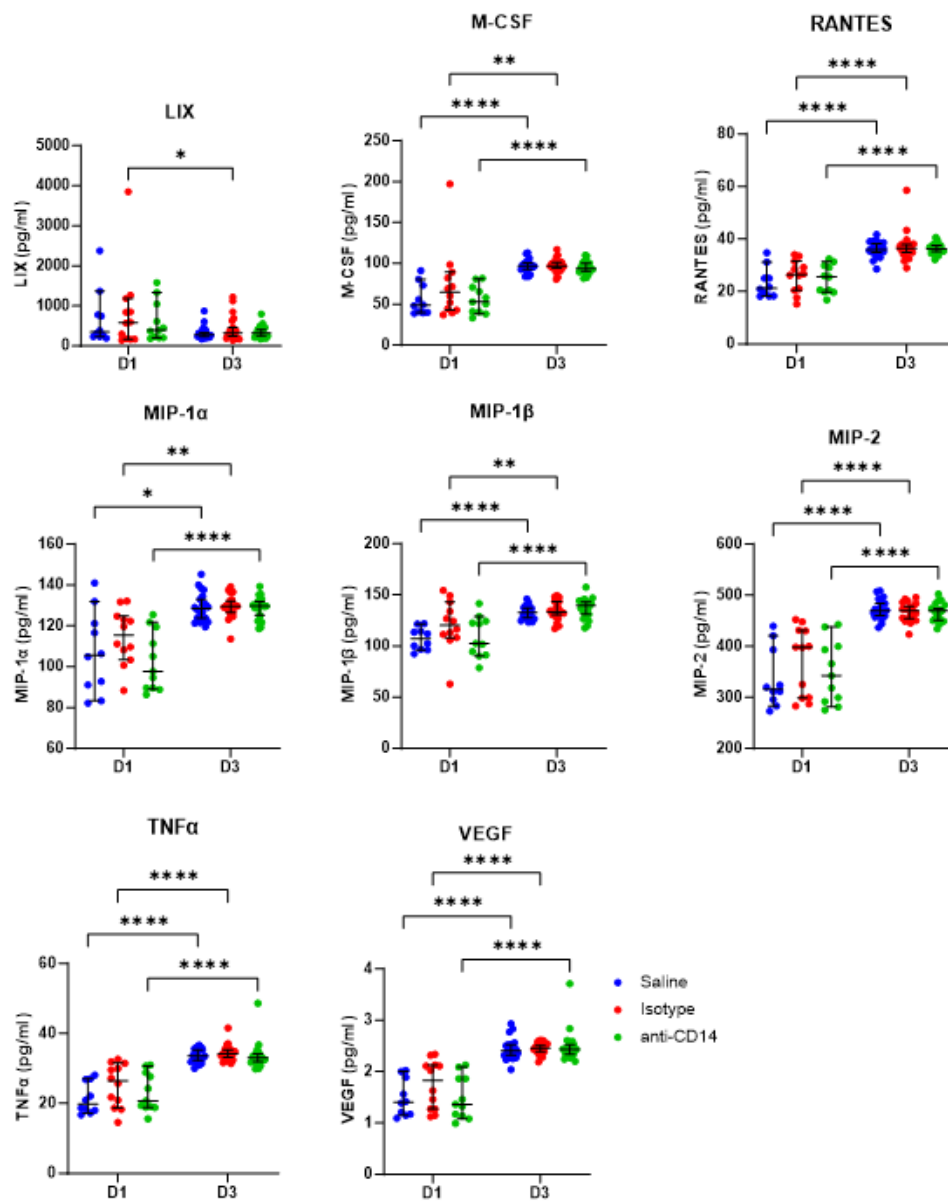
3 D3 post-STEMI. Mean \pm SEM. p<0.05, *** p<0.001, **** p<0.0001.



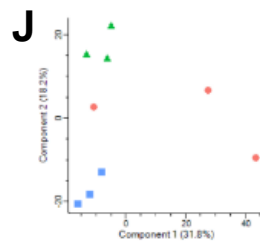
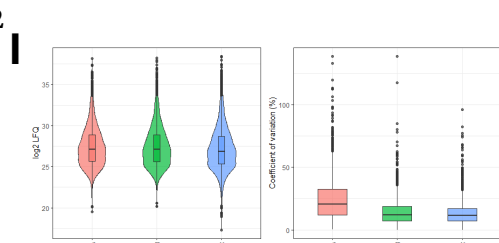
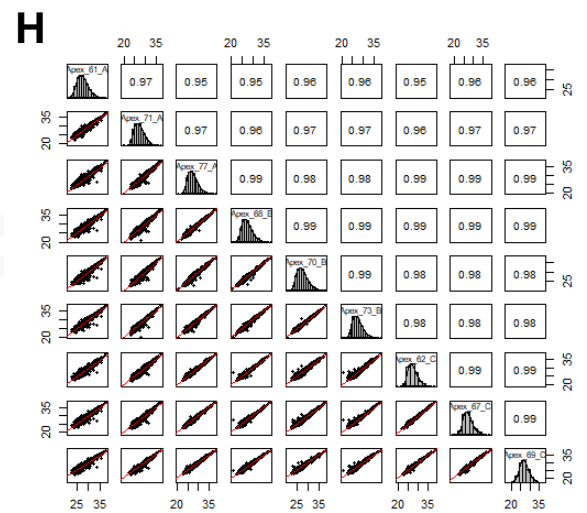
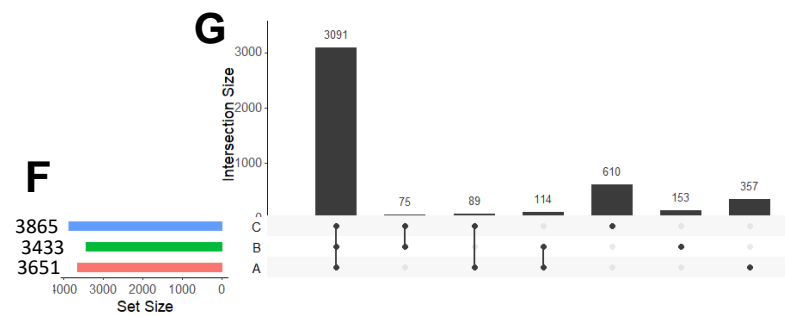
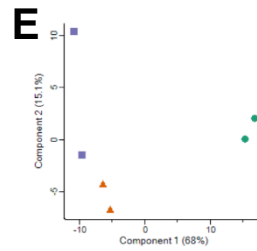
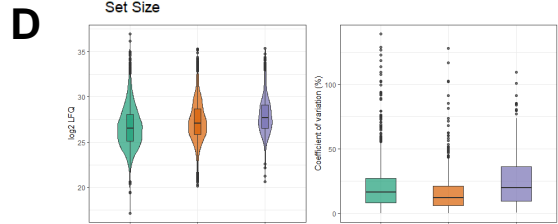
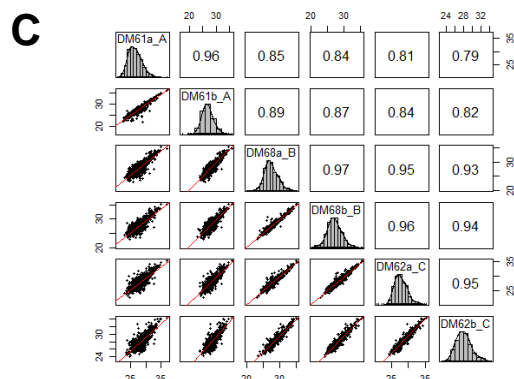
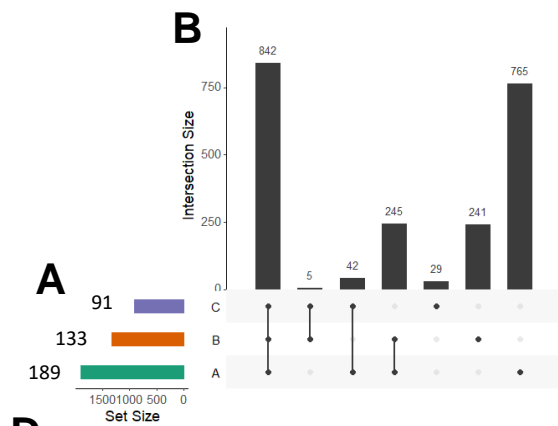
1

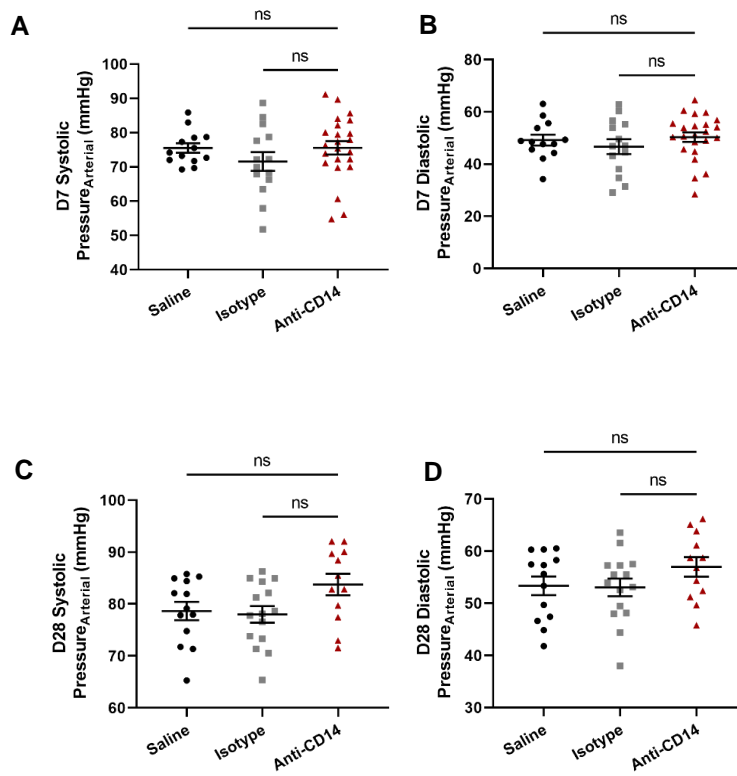
2 **Supplementary Figure S6. (continued) Circulating Growth Factors following CD14 Blockade at D1 and D3**

3 **post-STEMI.** Mean \pm SEM. **p<0.01, *** p<0.001, **** p<0.0001.



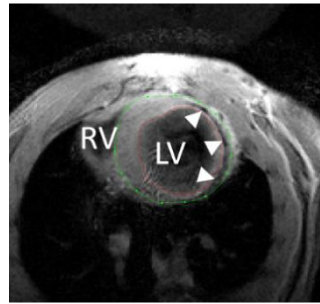
1
2 **Supplementary Figure S6. (continued) Circulating Growth Factors following CD14 Blockade at D1 and D3**
3 **post-STEMI. Mean ± SEM. * p<0.05, **p<0.01, **** p<0.0001.**





Supplementary Figure S8. Invasive arterial systolic and diastolic pressures measured at either 7 days (D7, A and B) or 28 days (D28, C and D) post-STEMI during pressure-volume (PV) catheterization. Mean \pm SEM. ns – not significant.

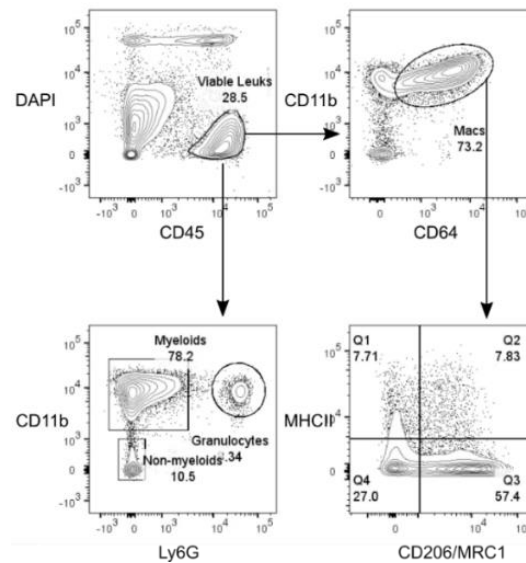
1



2

3 **Supplementary Figure S9. Cardiac magnetic resonance (CMR) imaging analysis example.** Endocardial borders
 4 of the left ventricle (LV) are traced at end-diastole and end-systole to determine fractional change (ejection fraction
 5 (EF%)). Epicardial borders are traced to define LV wall area (arrows). Note: After 21 days post-STEMI in this
 6 model, severe left ventricular free-wall thinning precludes accurate measurement of expanded infarct size.

7



8

9 **Supplementary Figure S10. Flow cytometry approach.** Antibodies for CD45, CD11b, CD64, CD14, MHCII, MRC1
 10 and Ly6G were used for sorting macrophages in flow cytometry experiments.